GEOPHYSICAL RESEARCH LETTERS, VOL. 18, NO. 1, PAGES 49-52, JANUARY 1991

PITCH ANGLE SCATTERING OF ENERGETIC PARTICLES BY OBLIQUE WHISTLER WAVES

U. S. Inan and T. F. Bell

Space, Telecommunications and Radioscience Laboratory, Stanford University, Stanford, CA 94305

Abstract. First order cyclotron or Landau resonant pitch angle scattering of electrons by oblique whistler waves propagating at large angles to the ambient field are found to be at least as large as that due to parallel propagating waves. Commonly observed precipitation of >40 keV electrons in association with ducted whistlers may thus be accompanied by substantial fluxes of lower energy (10 eV-40 keV) electrons precipitated by the nonducted components.

1. Introduction

Wave-induced precipitation of energetic electrons has long been recognized as a loss process for the radiation belts [*Kennel and Petschek,* 1966]. Recent ground-based observations of ionospheric effects of lightning-induced electron precipitation (LEP) bursts involving >40 keV electrons indicate that they occur commonly on L-shells of $2< L <3$ and are associated with ducted whistlers [*Inan and Carpenter,* 1987]. Theoretical modeling have so far only considered precipitation induced by ducted whistlers propagating parallel to the magnetic field [e.g., *Inan et al.,* 1989]. Although ducted VLF waves are common throughout the inner magnetosphere (L <6), most of the electromagnetic energy from ground-based sources propagates in the nonducted mode [*Edgar,* 1976; *Bell et al.,* 1981] and these oblique waves are in principle capable of strong interactions with energetic particles [*Bell,* 1986; *Shklyar,* 1986]. In this paper we apply the nonlinear motion equations derived by averaging over a gyroperiod [*Inan and Tkalcevic,* 1982; *Bell,* 1986] in a diffusion formulation to quantitatively estimate the first order cyclotron and Landau resonant scattering coefficients for arbitrarily oblique whistler-mode waves.

2. Gyro-averaged Diffusion Coefficients

Consider electrons in resonance with an oblique whistler wave, such that $v_R \simeq (n\epsilon\omega_H - \omega)k_\parallel^{-1}$, with $\epsilon = \sqrt{1-(v/c)^2}$, $k_\parallel = (\omega/c)\mu\cos\psi$ being the wave vector along $\overline{B}_0$, where ω_H is the electron gyrofrequency, ω is the wave frequency, μ is the refractive index, ψ is the wave normal angle, and n = 0,1 represents the Landau and first order gyroresonant conditions, respectively. The pitch angle diffusion coefficient, $D_{\alpha\alpha}$, is defined as $D_{\alpha\alpha} = <(\Delta\alpha)^2>/\Delta t$, where $\Delta t = (2\pi)^{-1}\Delta\omega(1 + v_R/v_{gz})$ is the average time particles stay in resonance, $\Delta\omega$ is the wave bandwidth, $v_{gz} = (\partial\omega/\partial k_z)$ [*Stix,* 1962], $\Delta\alpha$ is determined by the equations of motion [*Bell,* 1986] and the brackets <> represent averaging over Larmor phase. The rate of change of pitch angle for resonant electrons averaged over one gyroperiod is given by [*Bell,* 1986]

$$\frac{d\alpha}{dt} = -\frac{\omega_{\tau n}^2(1+\frac{\omega\cos^2\alpha}{n\epsilon\omega_H-\omega})}{k_z v_\perp}\sin\eta + \frac{v_\perp}{2\omega_H}\frac{\partial\omega_H}{\partial z} \qquad (1)$$

where $\omega_\tau^2 = \kappa\omega_{\tau_0}^2[J_{n-1}(\beta) - \alpha_1 J_{n+1}(\beta) + \alpha_2 J_n(\beta)]$ with $\omega_{\tau_0}^2 = (\epsilon q/2m_0)(B_x^w + B_y^w)k_z v_\perp$, $\beta = [n-\omega/(\epsilon\omega_H)]\tan\alpha\tan\psi$, $\kappa = [1+\omega^2/(c^2k_z^2)]$, $\epsilon = \sqrt{1-(v/c)^2}$, $\alpha_1 = (B_x^w - B_y^w)/(B_x^w + B_y^w)$ and $\alpha_2 = v_\perp^{-1}E_x^w/(B_x^w + B_y^w)$, with $J_i(\cdot)$ being the Bessel Function of the first kind and ith order and m_0 and q being particle rest mass and charge respectively.

Results for L = 2.5, a cold plasma density at the equator of N_{eq} = 1000 cm^{-3}, for electrons at the edge of the loss cone ($\alpha \simeq 12°$) and for a wave bandwidth of 200 Hz are shown in Figures 1, 2 and 3 for normalized frequencies $\Omega = f/f_{Heq}$ = 0.05, 0.25, and 0.5, where f_{Heq} is the electron gyrofrequency at the equator. As a means of normalizing our results, the wave components B_x^w, B_y^w and E_z^w at each ψ were computed for a Poynting Flux $S(\psi)$ equal to that for a ψ = 0° wave with $B_{x,y}^w$ = 1 pT at the equator.

The panels for each Ω show μ, the normalized gyroresonant (n=1) diffusion coefficient $\overline{D}^1(\psi)$=$D_{\alpha\alpha}^1(\psi)/D_{\alpha\alpha}^1(\psi = 0°)$,

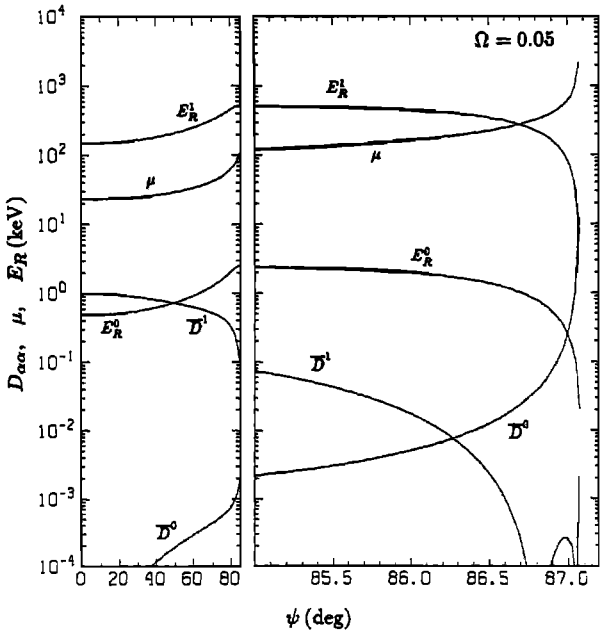

Fig. 1. Results for L = 2.5, N_{eq} = 1000 el/cc and Ω = 0.05 (2.8 kHz), showing the refractive index (μ), resonant electron energy for first order gyroresonance (E_R^1) and Landau resonance (E_R^0) and the normalized diffusion coefficients $\overline{D}^0$ and $\overline{D}^1$ as defined in the text. The $E_R^{0,1}$ values are plotted in keV on the same scale as the normalized quantities. The portion of the curves in the vicinity of the resonance cone is expanded for better illustration.

Paper number 90GL02476
0094-8534/90/90GL-02476$03.00

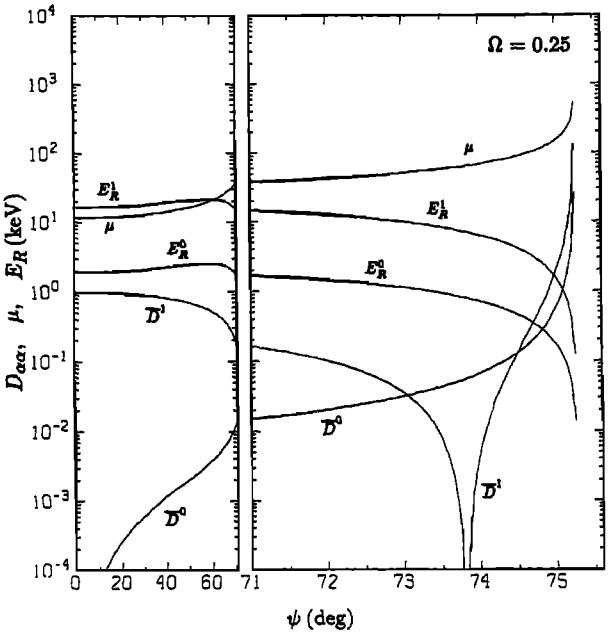

Fig. 2. Results for Ω = 0.25 (14 kHz). The format is identical to that of Figure 1.

the gyroresonant parallel energy E_R^1, and the same quantities for Landau (n=0) resonance ($\overline{D}^0(\psi)$ and $E_R^0(\psi)$). The $D_{\alpha\alpha}^0$ is normalized to that for gyroresonance (n=1) at ψ=0°, so that $\overline{D}^0(\psi)=D_{\alpha\alpha}^0(\psi)/D_{\alpha\alpha}^1(\psi=0°)$, noting that $D_{\alpha\alpha}^0$ (ψ=0°)=0 for ψ=0°. The numerical values of $D_{\alpha\alpha}^1$ (ψ=0°) for the cases shown were 0.04, 0.23, and 0.53 deg^2/s respectively for Ω=0.05, 0.25, and 0.5.

The cold plasma formulation used here is sufficiently accurate as long as $c(\mu\cos\psi)^{-1} \gg v_{th}$ and $k_\perp v_{th} \ll w_H$, where v_{th} is the velocity of thermal electrons and $k_\perp$ is the wave vector perpendicular to $\overline{B}_0$ [*Sazhin and Sazhina*, 1985], conditions which were satisfied for the smallest wavelengths (i.e., highest values of μ) considered in Figures 1-3.

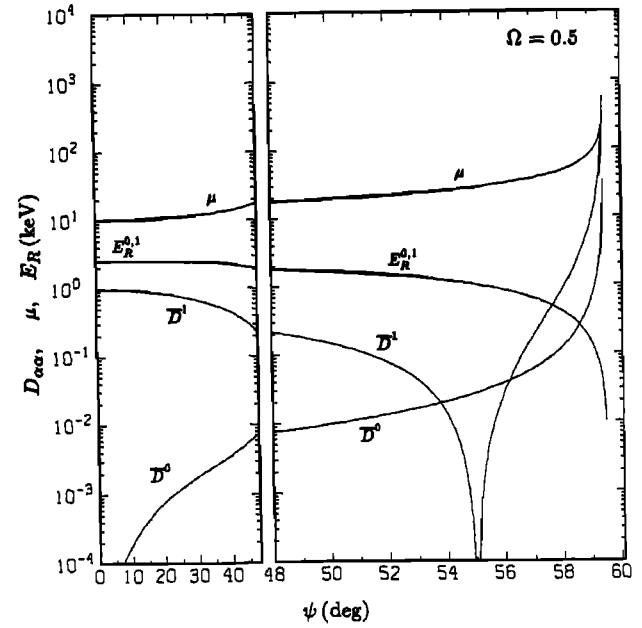

Fig. 3. Results for Ω = 0.5 (28 kHz). The format is identical to that of Figure 1.

For Ω = 0.05, E_R^1 and E_R^0 rapidly decrease as ψ approaches the resonance cone angle ψ_r [*Stix*, 1962] since $k_\parallel$ becomes large leading to resonance with slower particles. Although $\overline{D}^0$=0 for ψ=0°, it does increase steadily with ψ, due to the scattering mainly by E_z^ω for small ψ, but also by $B_{x,y}^\omega$ as ψ increases [*Inan and Tkalcevic*, 1982]. As $\psi \to \psi_r$, $\overline{D}^0$ increases due to the enhanced electric field intensities (per unit S(ψ)) of this quasi-electrostatic wave, with $\overline{D}^0 \simeq 1$ for ψ within < 0.1° of ψ_r. For Ω = 0.05 $\overline{D}^1$, decreases with ψ and goes through minima ($\overline{D}^1$=0 due to ω_r=0 as opposing effects of the different wave components cancel [*Bell*, 1986]) and $\overline{D}^1(\psi \sim \psi_r) \ll \overline{D}^1(0)$ even for the highest value of ψ considered .

With $S(\psi)$ normalized to that for a 1 pT wave with ψ = 0°, the intensity of the E_z^ω and B_x^ω components at the highest ψ (ψ=87.08°) in Figure 1 are 0.06 mV/m and 0.018 pT, respectively. The transverse wave electric component $|E_x^\omega| \simeq |E_z^\omega|(\cos\psi)^{-1} \simeq 1.2$ mV/m for $\psi \simeq \psi_r$, as compared with $E_x^\omega \simeq 0.013$ mV/m for a ψ = 0° wave with $\mu \simeq 23$ and B_ω^x=1 pT. Thus, the enhanced scattering for $\psi \simeq \psi_r$ is in part due to the higher values of the wave electric field resulting from our assumption of $S(\psi)$=const.. The larger $D_{\alpha\alpha}$ values for $\psi \simeq \psi_r$ are also partly due to the fact that v_{gz} for ψ=87.08° is only 3% of that ψ=0°, since $D_{\alpha\alpha}$ are proportional to the resonance time, Δt.

Oblique wave scattering is large over a wider range of ψ for Ω = 0.25 (Figure 2). The first and only minimum in $\overline{D}^1$ occurs at $|\psi - \psi_r| \simeq 1°$ after which $\overline{D}^1$ rapidly increases with ψ and is $\gg 1$ for $\psi \simeq \psi_r$. First order gyroresonant scattering by oblique waves with $|\psi - \psi_r| < 1°$ could thus be at least as large as that due to field aligned (ψ=0°) waves. We note that E_R^1 also varies rapidly as $\psi \to \psi_r$, so that, for example, for $|\psi - \psi_r| < 0.1°$, significant gyroresonant scattering of <100 eV electrons can be expected whereas E_R^1 for ψ=0° is ~2 keV. The Landau resonant scattering also appears to be significant over a wider range of ψ for Ω=0.25 since $\overline{D}^0$ is comparable to $\overline{D}^1$ for $\psi \simeq \psi_r$. The E_R^0 are even lower so that scattering of <10 eV electrons can be expected for $|\psi - \psi_r| < 0.1°$. The E_R^0 for the highest value of ψ considered (ψ=75.23°) is ~10 eV so that the cold plasma model is still valid in the sense discussed above. At this ψ we have E_z^ω=0.1 mV/m and B_x^ω=0.045 pT, and v_{gz} is ~3% of that for ψ = 0°.

Oblique wave scattering is significant over an even wider range of ψ for Ω=0.5 (Figure 3); $\overline{D}^1$ >0.1 for $|\psi - \psi_r| <$ 3° and $\overline{D}^1$ >1 for $|\psi - \psi_r|$ <1.8°. For example, the $D_{\alpha\alpha}^1$ for ~100 eV electrons resonant with waves having $\psi \simeq 59°$ ($|\psi - \psi_r \simeq 0.5°$) is 10 times higher ($\overline{D}^1$=10) than that for 2.5 keV electrons resonant for ψ=0°. The Landau resonant scattering also appears to be relatively more significant for Ω=0.5 although less so than gyroresonant scattering. We note that $\overline{D}^0 \simeq 0.1\overline{D}^1$ over the range $|\psi - \psi_r| < 3°$ and that $E_R^1 = E_R^0$ for Ω=0.5. First order gyroresonant scattering is dominant in this frequency regime for oblique waves with $|\psi - \psi_r| <3°$. We note also that $E_R^0 = E_R^1 > 1$ eV for the highest value of ψ considered (ψ=58.02°), so that the cold plasma approximation is again valid. The intensity of the wave components at this ψ are E_z^ω=0.02 mV/m and B_x^ω=0.041 pT, and v_{gz} is 2% of that for ψ = 0°.

3. Typical Raypaths and Wave Normal Distributions

Figures 1-3 show that the $D_{\alpha\alpha}^{0,1}$ exhibit strong dependence on ψ, especially as $\psi \rightarrow \psi_r$. The use of the cold plasma resonance cone has physical significance since thermal corrections are unimportant for the wavelengths considered [*Sazhin and Sazhina*, 1985]. Nevertheless, the importance of our results needs to be assessed in the context of a realistic model of the oblique wave propagation in the magnetosphere and the resulting wave normal distribution.

Results of raytracing in a model magnetosphere (Figure 4) for Ω=0.05, 0.25, and 0.5 are shown in Figure 5. The lowest panel shows the raypaths in a magnetic meridional plane for Ω=0.5 whereas the upper panels show $Y=|\psi-\psi_r|$ for different Ω at the equatorial crossings for rays injected at 1000 km altitude on different L-shells. For Ω=0.05, $\psi \rightarrow \psi_r$ after the first few equatorial crossings although the initial behaviour of rays injected at higher L-shells is complicated by reflections from the plasmapause [*Jasna et al.*, 1990]. At L=2.5 ($D_{\alpha\alpha}^{0,1}$ calculated in section 3), Y ranges from 0.5° for injection at L=1.5 to as low as 0.03° for injection at L=4, indicating that relatively large $\overline{D}^0$ (ψ within <0.1° of ψ_r) can be attained for 2.8 kHz rays that enter the medium at $L < 3$. Although such ψ are achieved only after 5-6 bounces of the wave packet, this type of propagation is known to commonly occur within the plasmasphere [*Edgar*, 1976].

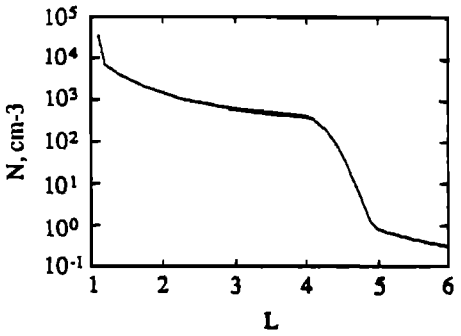

Fig. 4. Equatorial electron density profile used in raytracing calculations. The cold plasma distribution along the field lines was assumed to be in diffusive equilibrium.

For Ω =0.25 (14 kHz), the first equatorial crossing occurs for a ray that enters the medium at an L-shell between L=1.5 and 2 but with $Y \simeq 10$. For rays injected at L=2 and 2.5, the second equatorial crossings occur at L <2.5 and the ray injected at L=3 does not undergo reflection. However, noting that the precise layout of paths is dependent on the cold plasma gradients we can expect the second crossing (with Y <1°) to be near L=2.5 under some conditions. In such cases, $\overline{D}^{1,0} > 1$ may be attained.

For Ω=0.5 (28 kHz) rays injected over a wide range of latitudes focus together and cross the equator near L=2.5, and $\psi \rightarrow \psi_r$ with increasing injection latitude. Since $\overline{D}^{1,0} > 1$ for ψ within <1.8° of ψ_r (Figure 3), significant scattering would be induced at L = 2.5 by 28 kHz waves injected at L >2.5. While the $\overline{D}^{1,0}$ appear to increase without limit as injection occurs at higher latitudes and $\psi \rightarrow \psi_r$ near the equator, we note that eventually Landau damping will come into play as E_R^0 decreases below about 1 eV, when the condition $c(\mu \cos\psi)^{-1} \geq v_{th}$ no longer holds. In summary, for any given L-shell (frequency), the most efficient equatorial scattering is expected for frequencies (L-shells) such that $\Omega \simeq 0.5$, for two reasons; (i) the range of ψ for which $\overline{D}^1$ and $\overline{D}^0$ are

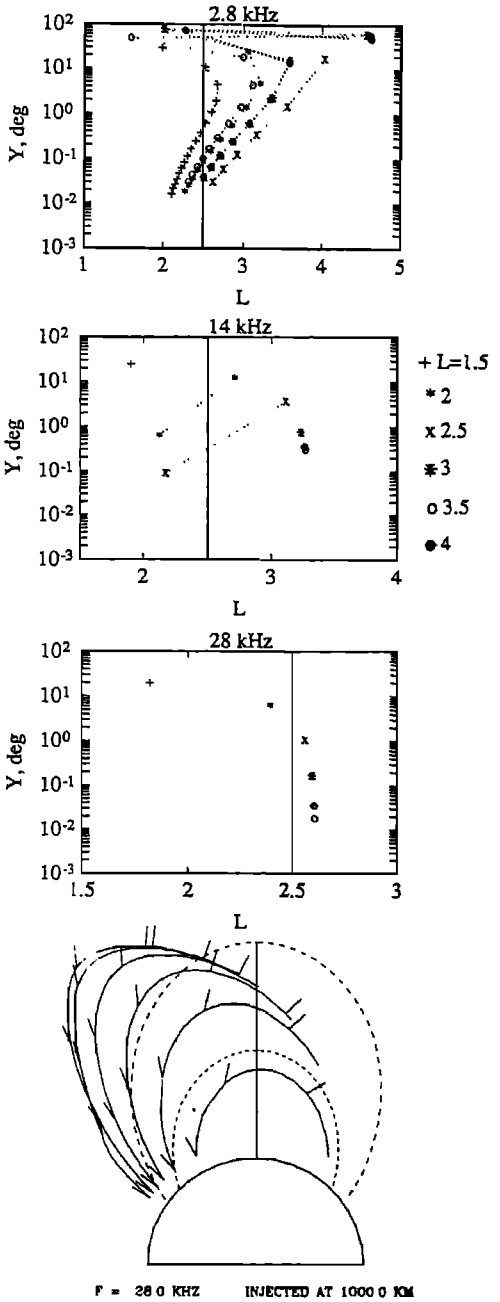

Fig. 5. The top three panels show $Y = |\psi - \psi_r|$ at the equatorial crossings of the different rays injected at 1000 km altitude on L-shells of L=1.5, 2, 2.5, 3, 3.5, 4 at each of the three frequencies used, namely 2.8, 14, and 28 kHz. Each point with a different symbol represents a ray injected at a different L-value as indicated in the inset. Rays injected at higher and higher latitudes cross the equator with smaller and smaller values of Y. The distribution of the actual raypaths in a meridional plane for the 28 kHz case are given in the bottom panel. The wave normal direction is indicated at regular intervals along the path by a short line at the appropriate angle.

>1 is wider (Figure 3), and (ii) ψ is closest to ψ_r for a wider range of entry locations of the wave energy into the medium (Figure 5).

4. Summary and Discussion

Cyclotron and Landau resonant pitch angle scattering induced by oblique whistlers with $\psi \simeq \psi_r$ can be at least as large as that due to parallel propagating waves. Raytracing studies indicate that these relatively high wave normal angles are attained in a variety of different modes depending on wave frequency and point of entry to the magnetosphere. Observed LEP events involving >40 keV electrons and attributed to whistler components propagating along the magnetic field lines [*Inan and Carpenter*, 1987] should thus be accompanied by substantial fluxes of 10 eV-40 keV electrons scattered by the oblique whistler components launched by the same lightning discharges.

Although there currently are no reported observations of such low energy precipitation associated with lightning-generated whistler waves, the ground-based VLF remote sensing technique commonly used to study LEP events is sensitive only to the high energy component (>40 keV) of the precipitation that penetrates to D-region altitudes [*Inan and Carpenter*, 1987]. Energetic particle measurements on satellites require exceptionally high time resolution (<1 s) in order to identify LEP bursts [*Voss et al.*, 1984]. Measurements on the S81-1 satellite did have sufficient resolution and sensitivity but only for >6 keV [*Voss et al.*, 1984]. Lower energy electron data from other spacecraft may exist and should be analyzed in search for effects predicted here.

The precipitated energy flux levels from these interactions would depend on the whistler intensity, trapped particle distribution, and other parameters, and need to be estimated by including the effects of a full distribution of particles interacting with the wave at different points along the field lines as has been done for interactions with ducted whistlers [*Inan et al.*, 1989]. There are at least two reasons to expect the energy fluxes precipitated to be relatively high. Firstly, the scattering coefficients can often be higher than that for parallel propagating waves as described above. Secondly, the available trapped fluxes at the lower energies are higher for most magnetospheric particle distributions. If precipitation of significant fluxes of 10 eV-40 keV electrons can be induced by individual oblique whistler components, we can expect generation and maintenance of secondary ionization enhancements at altitudes of 200-300 km, possibly leading to the formation of whistler 'ducts' via upward diffusion. Similar effects would be expected in association with VLF transmitters, since observed wave power levels are comparable to whistlers in the frequency range of 10-25 kHz. For a given wave frequency, strongest effects would be expected in the vicinity of the equator on the L-shells corresponding to $\Omega \simeq 0.5$.

Acknowledgements. This research was supported by National Aeronautics and Space Administration under grant NAGW-1582. We thank D. Jasna for her help with Figure 5 and Zheng Xu for her typesetting of the manuscript.

References

Bell, T. F., U. S. Inan, and R. A. Hellwell, Nonducted coherent VLF waves and associated triggered emissions observed on the ISEE-1 satellite, *J. Geophys. Res., 86*, 4649, 1981.

Bell, T. F., The wave magnetic field amplitude threshold for nonlinear trapping of energetic gyroresonant and landau resonant electrons by nonducted VLF waves in the magnetosphere, *J. Geophys. Res., 91*, 4365, 1986.

Edgar, B. C., The upper and lower frequency cutoffs of magnetically reflected whistlers, *J. Geophys. Res., 81*, 205, 1976.

Inan, U. S., and S. Tkalcevic, Nonlinear equations of motion for Landau response interacitons with a whistler mode wave, *J. Geophys. Res., 87*, 2363, 1982.

Inan, U. S., and D. C. Carpenter, Seasonal, latitudinal and diurnal distributions of whistler-induced precipitation events, *J. Geophys. Res., 92*, 3293, 1987.

Inan, U. S., M. D. Walt, H. D. Voss, and W. L. Imhof, Energy spectra and pitch angle distributions of lightning-induced electron precipitation: analysis of an event observed on the S81-1 (SEEP) satellite, *J. Geophys. Res., 94*, 1379, 1989.

Jasna, D., U.S. Inan, and T.F. Bell, Equatorial gyroresonance between electrons and magnetosphericaly reflected whistlers, *Geophys. Res., Lett., 17*, 1865, 1990.

Kennel, C. F., and H. E. Petschek, Limit on stably trapped particle fluxes, *J. Geophys. Res., 71*, 1, 1966.

Sazhin, S. S., and E. M. Sazhina, Quasielectrostatic whistler mode propagation, *Planet. Space Sci.,33*, 295, 1985.

Shklyar, D. R., Particle interaction with and electrostatic VLF wave in the magnetosphere with an application to proton precipitation, *Planet. Space Sci.,34*, 1091, 1986.

Stix, T.H., *The theory of plasma waves*, McGraw Hill, New York, 1962.

Voss, H. D., W. L. Imhof, J. Mobilia, E. E. Gaines, M. Walt, U. S. Inan, R. A. Helliwell, D. L. Carpenter, J. P, Katsufrakis, H. C. Chang, Lightning-Induced Electron Precipitation, *Nature, 312*, 740, 1984.

U. S. Inan and T. F. Bell, Space, Telecommunications And Radioscience Laboratory, Department of Electrical Engineering/SEL, Stanford University, Stanford, CA 94305.

(Received September 19, 1990;
revised October 23, 1990;
accepted November 5, 1990)